

# IMPACT OF WELDING PROCEDURES ON THE MECHANICAL ATTRIBUTES, STRESS CORROSION BEHAVIOR AND MICROSTRUCTURE FEATURES OF AUSTENITIC STAINLESS STEEL JOINTS

Amit Kumar Patel<sup>1</sup>, Dr. A. S. Verma<sup>2</sup>,

<sup>1</sup>M.Tech. Mechanical Engineering Scholar, Department of Mechanical Engineering, B. N. College of Engineering and Technology

<sup>2</sup>Professor, Department of Mechanical Engineering, B. N. College of Engineering and Technology  
Lucknow, Uttar Pradesh, India

**Abstract**— The high molybdenum grades of austenitic stainless steels such as 316, 316L, 317 and 316LN are used for the fabrications of chemical storage tanks, pressure vessels and structural components of nuclear reactors. The presence of nitrogen in the 316LN grade provides good mechanical properties at high temperatures ( $> 427$  O C), hence it is successfully used in the development of the fast breeder reactors. Also, the presence of a very low weight percentage of carbon (0.026 %) content is capable to eliminate sensitization related issues during the welding process and gives resistance to the Intergranular Corrosion (IGC) during its services. This research work explores the effect of different welding processes namely Gas Tungsten Arc Welding (GTAW), Activated flux Gas Tungsten Arc Welding (AGTAW), Laser Beam Welding (LBW) and Friction Stir Welding (FSW) on the weld thermal cycles, microstructures, mechanical properties and stress corrosion cracking behavior on 316LN welded joints. The weld joints of 316LN base plates with the dimension of 75 mm x 300 mm x 3 mm were fabricated using the above mentioned four welding techniques. The major parameters namely current (65 A), voltage (12 V) and welding speed (60 mm/min) were used to fabricate GTAW joints. The major parameters namely current (120 A), voltage (12.6 V) and welding speed (85 mm/min) were used to fabricate AGTAW joints. The major parameters namely power (2.5 kW) and welding speed (1500 mm/min) were used to fabricate LBW joints. The major parameters namely tool rotational speed (600 rpm), vertical thrust force (14 kN) and traverse speed (50 min/mm) were used to fabricate FSW joints.

**Index Terms**—316LN grade steel, Gas Tungsten Arc Welding (GTAW), Activated flux Gas Tungsten Arc Welding (AGTAW), Laser Beam Welding (LBW) and Friction Stir Welding (FSW).

## I. INTRODUCTION

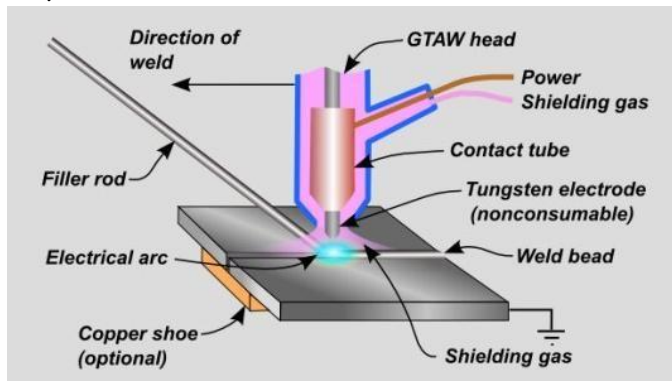
### A. AUSTENITIC STAINLESS STEEL 316LN WELDING

In general, the 316LN austenitic grade is extremely weldable, and the inclusion of Ni stabilises the austenite phase and, in many circumstances, keeps the toughness of the base metal after welding. Nevertheless, in certain instances, the metastable  $\delta$ -ferrite persists throughout the rapid cooling cycles, leading to a little decrease in toughness in the 316LN grade. Intergranular Corrosion (IGC) assaults are avoided and the production of Cr<sub>23</sub>C<sub>6</sub> at grain boundaries during weld heat cycles is avoided due to the low carbon content. However, because to the increase in dendritic size during Post-Weld Heat Treatments (PWHT), there is a little chance of the IGC in 316LN grade (Xin et al. 2018). The 316LN welded joints are protected against the development of Cr<sub>2</sub>N precipitate at the weld zone by the strong solubility propensity of the nitrogen in the austenite phase. The mechanical qualities of the 316LN weld joint, created by the narrow gap metal active gas arc welding (NG-MAG) technique, were superior to those of the base metal. Additionally, 1.0 kJ/mm to 1.4 kJ/mm was determined to be the appropriate heat input to achieve welding without defects (Wenkai et al. 2015). Because of the multiple heat cycles, multi-pass tungsten inert gas welding causes increased residual stress in 316LN weld zones (Vasantharaja et al. 2015). The 316LN joint, which was welded using an electron beam, exhibited a fusion zone hardness that was about 40% harder than base metal because of the fine dendritic microstructural morphology. This is explained by the fact that this specific process solidifies quickly (Joseph et al. 2012). In this inquiry, 316LN SS was joined using the procedures of Gas Tungsten Arc Welding (GTAW), Activate flux Gas Tungsten Arc Welding (AGTAW), Laser Beam Welding (LBW), and

Friction Stir Welding (FSW). The sections that follow provide a quick overview of these procedures.

**B. GAS ARC WELDING TUNGSTEN (GTAW)**

Austenitic stainless steel sheets and plates are often joined using the GTAW method and the appropriate filler materials (Berenjani et al. 2014, Buddu et al. 2014). A welding torch or head with a non-consumable tungsten electrode and shielding gas arrangements is used in this joining operation (Figure 1.1). A layer of shielding gas, such as argon or helium, keeps oxygen and nitrogen from contacting the molten metal during the joining process, preventing them from entering the weld pool. The non-consumable tungsten electrode and the base metal form an electric arc. The electric arc provides the thermal energy needed to melt and fuse the base metals together. This method limits the weld pool penetration to around 3 mm in a single pass.

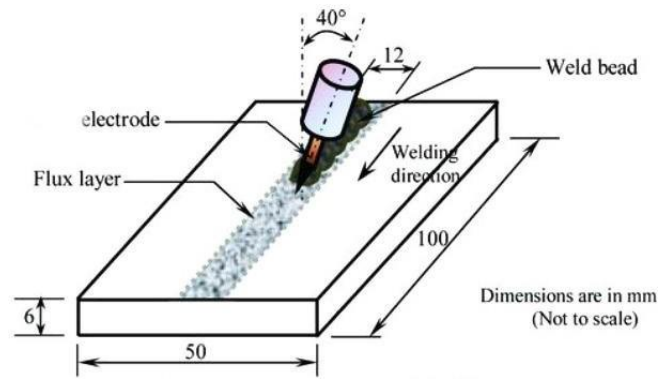


(Source: Cary et al. 2005)

Figure 1.1 Schematic diagram of the gas tungsten arc welding process

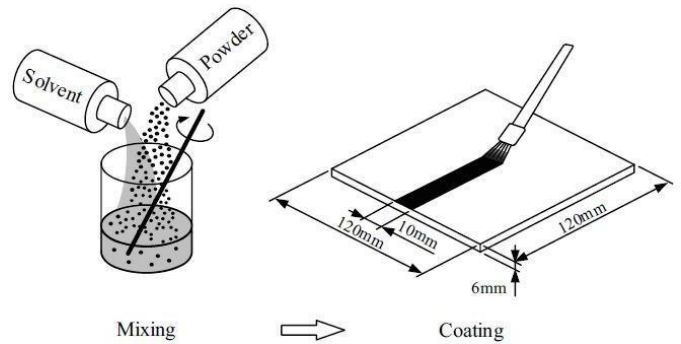
**C. ACTIVATED FLUX GAS TUNGSTEN ARC WELDING (AGTAW)**

The AGTAW procedure follows the same guidelines and configurations as the GTAW procedure. Between the base metal and the non-consumable tungsten electrode, an electric arc is also created in this instance. The heat energy generated by the electric arc facilitates the melting and connecting of the base metals. The distinction is that in this technique, no filler material is used (Figure 1.2), and the base metal is coated with activated flux (single or multi-compound) before the joining process. When compared to the GTAW technique, the weld pool penetration increased due to the effect of reverse marangoni convection. In comparison to the GTAW method, this procedure produces three times the weld penetration. Figure 1.3 shows how activated flux is prepared and coated on the base metal. Stainless steels are joined together using the following common fluxes: (i) Cr<sub>2</sub>O<sub>3</sub>; (ii) TiO<sub>2</sub> SiO<sub>2</sub>; (iv) CuO; and (v) NiO (Tseng et al. 2017, Vasudevan 2017).



(Source: Tathgir et al. 2015)

Figure 1.2 Schematic diagram of the activated flux gas tungsten arc welding process

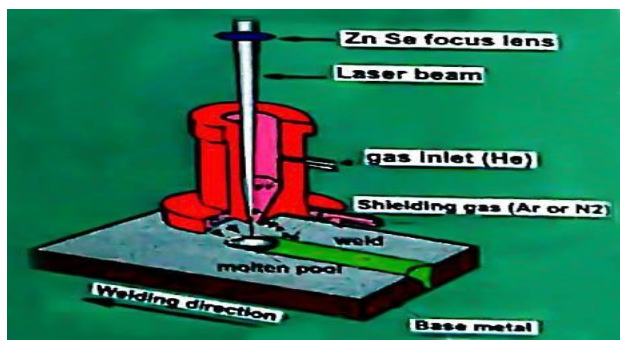


(Source: Tseng et al. 2012)

Figure 1.3 Preparation and coating of activated flux on the base metal prior welding process

**D. LASER BEAM WELDING (LBW)**

Figure 1.4 displays the schematic diagram for the LBW process. Heat energy density is produced by the high power monochromatic laser source and is utilised in the LBW process to melt and fuse (fusion weld) the base metals. Owing to the intense, narrow laser beams, this process will produce a very small weld bead with a high penetration depth. The automobile sector makes great use of this technology due to its quicker welding speed. Many austenitic SS grades, such as 316L, 304L, and 321 are successfully joined by the LBW process (Chukkanet al. 2015, Kuryntsev et al. 2015, Koseet al. 2016 & Rong et al. 2017).

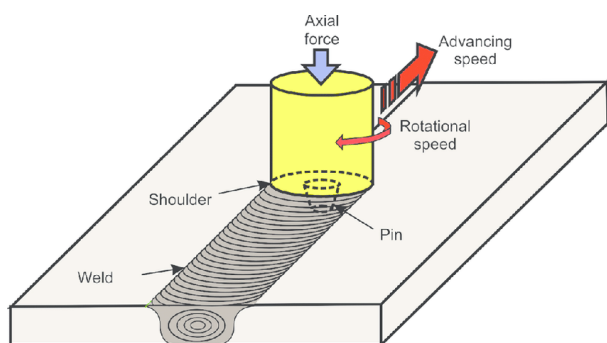


(Source: Chen et al. 2000)

Figure 1.4 Schematic diagram of the laser beam welding process

### E. FRICTION STIR WELDING (FSW)

Originally developed at The Welding Institute (TWI) in 1991, FSW is a solid-state metal joining process that was extensively utilised for welding aluminium alloys (Thomas et al. 1991). Afterwards, connecting steel and stainless steel is a common use for this approach (Lakshminarayanan et al. 2010). Figure 1.5 displays the FSW process schematic diagram. Inserted at the neighbouring edges of the parent metal, a high-speed, non-consumable rotating tool with two principal parts (a shoulder and a pin) is traversed over the interface of the two metals to be connected (Mishra et al. 2005). The base metal is initially pushed into the plastic state and softened by the frictional heat created by the physical contact between the tool and base metal. Furthermore, the pin's stirring action stirs a huge volume of base metals together in a solid state, causing severe plastic deformation with dynamic recrystallization and the creation of tiny grains at the weld zone. High mechanical qualities are provided by the fine grains in comparison to the parent metal and weld connections made using traditional welding methods. Since shielding gas is not used for this process and no filler material is needed, it is considered a green technique in the material joining industry. Because the metal is bonded below its solidus temperature, this method arrests the flaws that arise as a result of solidification (fusion welding).



(Source: Fraser et al. 2015)

Figure 1.5 Schematic diagram of the friction stir welding process

## II. LITERATURE REVIEW

Because of its excellent mechanical and corrosion resistance qualities, austenitic stainless steel (Austenitic SS) grades are frequently employed in the chemical industry and nuclear reactor advancements. Depending on the type of technique and the parameters utilised, the fabrication processes may have positive or negative effects on certain qualities. This chapter provides a detailed discussion of the mechanical attributes, stress corrosion cracking behaviour, and microstructural features of various Austenitic stainless steel welded joints. For the literature review, the following welding procedures on the various Austenitic SS grades were included: (i) Activated flux (ii) Gas Tungsten Arc Welding (GTAW) or Tungsten Inert Gas Welding (TIG) (iii) Laser Beam Welding (LBW) (iv) Gas Tungsten Arc Welding (AGTAW) (v) Electron Beam Welding (EBW) (vi) Gas Metal Arc Welding (GMAW) or Metal Inert Gas Welding (MIG) (vii) Friction Stir Welding (FSW) (viii) Metal Arc Laser Welding; (ix) TIG/Laser Hybrid Welding.

The key findings from a thorough review of the literature on the microstructural traits, mechanical attributes, and stress corrosion cracking behaviour of austenitic stainless steel weld joints are outlined. Numerous studies were conducted to evaluate the mechanical and microstructural characteristics of the weld joints between the austenitic stainless steel grades 304L and 316L. The following is a summary of the main ideas covered in the literature on welding Austenitic stainless steel grades. (i) There aren't many studies on the joining of nuclear grade austenitic stainless steel (316LN) that is nitrogen enhanced and low in carbon. (ii) There is literature available for the EBW method that discusses connecting 316LN by greater energy density welding, but there is none for the LBW technique. (iii) There isn't a study on the mechanical and microstructural features of the 316LN SS joint made using the solid-state welding (FSW) technology that is currently accessible. (iv) No research article exists that evaluates the SCC behaviour of the 316LN SS grade weld joints. A thorough research strategy is outlined in this examination to examine the impact of the welding techniques (GTAW, AGTAW, LBW, and FSW) on the microstructural features, mechanical attributes, and stress corrosion cracking behaviour of austenitic stainless steel 316LN welded joints.

## III. OBJECTIVES

The main objectives of the present investigation are:

- Evaluating the impact of the various welded joints' mechanical qualities, such as (i) tensile properties, (ii) impact toughness, (iii) microhardness across the weld zones, and (iv) bend properties, on the welding methods (GTAW, AGTAW, LBW, and FSW).

#### IV. EXPERIMENTAL WORK

##### A. INTRODUCTION

This study's main goal is to evaluate the microstructural morphologies of AISI 316LN Austenitic Stainless Steel weld joints made using the following processes: (i) Gas Tungsten Arc Welding (GTAW); (ii) Activated Gas Tungsten Arc Welding (AGTAW); (iii) Laser Beam Welding (LBW); and (iv) Friction Stir Welding (FSW).

The current inquiry followed the following order of work:

(i) An assessment of the base metal's principal mechanical attributes, including Yield Strength (YS), Ultimate Tensile Strength (UTS), Percentage of Elongation, Impact toughness, and Microhardness (Vickers).

(ii) 316LN weld joint fabrication utilising LBW, FSW, AGTAW, and GTAW procedures.

(iii) Testing the 316LN Austenitic Stainless Steel weld joints for tensile, impact toughness, microhardness, and bend characteristics in accordance with ASTM guidelines.

##### B. BASE METAL PROPERTIES EVALUATION

The hot-rolled, 3 mm-thick AISI 316LN Austenitic Stainless Steel was used as the foundation metal for this inquiry. A vacuum arc emission spectrometric method was used to examine the base metal's chemical makeup. The WDS method was used to determine the quantity of nitrogen. This analysis is conducted at several base metal sites, and Table 4.1 provides the average value of the weight percentage of the elements.

Table 4.1 Chemical composition of the 316LN base metal

Material	Weight percentage of elements									
	Cr	Ni	Mo	Mn	Si	C	S	P	N	Fe
AISI 316LN	17.800 ± 0.250	11.700 ± 0.380	2.400 ± 0.100	1.600 ± 0.150	0.450 ± 0.080	0.026 ± 0.005	0.009 ± 0.001	0.026 ± 0.007	0.095 ± 0.006	bal

Figure 4.1 shows the dimensions of tensile samples of the base metal that were manufactured in accordance with ASTM E8-04 (ASTM, 2004) standards. The 50 kN Universal Testing Machine (Bluestar manufacture, Model: LDW 50) was used to test the base metal's tensile strength at room temperature and a crosshead speed of 2 mm/min. in the gauge section, the base metal was stretched preferentially, and in the gauge portion's

centre, necking and fracture took place. The load versus displacement data was recorded, and those recorded values were used to produce the base metal's stress vs strain diagram. The values for the base metal's yield strength, ultimate tensile strength, and percentage of elongation are reported in Table 4.2.

Table 4.2 Mechanical properties of the base metal (Measured)

Base Metal	AISI 316LN SS
Yield strength (MPa)	309.0 ± 7.0
Tensile strength (MPa)	616.0 ± 4.0
Elongation (%) in 25 mm gauge length	64.3 ± 1.2
Vicker's Micro-hardness (HV <sub>0.5</sub> @ 15 sec)	185.0 ± 5.0
Charpy Impact Toughness @ RT (J)(sub size)	54.0 ± 1.9

Using a pendulum-style Charpy impact test machine (FIE manufacture, Model: IT30) at room temperature, the impact toughness of the base metal was assessed. This specific machine has a maximum capacity of 300 J. The subsize samples were manufactured in accordance with ASTM E23-07

(ASTM, 2007) criteria using a base metal with a thickness of 3 mm. In Figure 4.2, the sample dimensions are displayed. Three base metal samples were fractured, and the absorbed energy (also known as impact toughness) was measured. The average result is shown in Table 4.2.

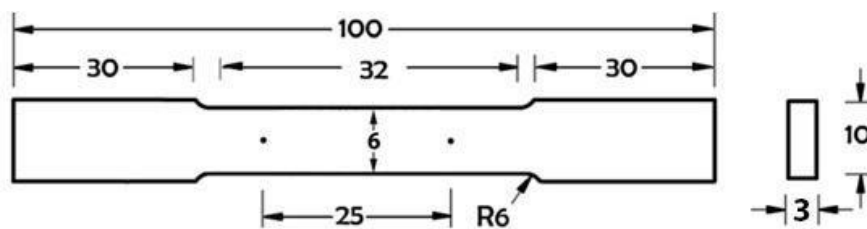
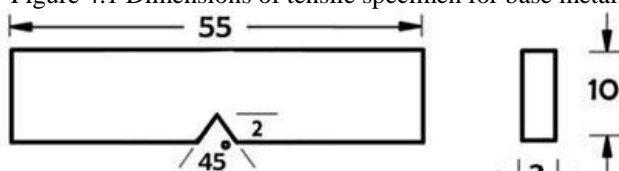


Figure 4.1 Dimensions of tensile specimen for base metal



All dimensions are in "mm"

Figure 4.2 Dimensions of impact specimen for base metal

Vicker's microhardness testing apparatus (ESEWY manufacture, Model: EW-423DAP) was used to measure the base metal's hardness at a load of 0.5 kg and a dwell duration of 15 s. I Optical microscopy (Olympus make, Model: BX 51M) and scanning electron microscopy (ZEISS make, Model: EVO 18 research) were used to examine the microstructural morphology of the base metal. When annealing twins were present, the base metal showed full austenite phase. It was found that the base metal's average grain size was 54  $\mu\text{m}$ .

### C. FABRICATION OF WELD JOINTS

For the necessary joint fabrications, a base plate of 300 mm in length, 75 mm in width, and 3 mm in thickness was machined. The V-groove edge was ready for the second pass GTAW procedure with an incorporated angle of 60 degrees

Celsius. This V-groove was primarily used to execute two passes on the same side of the 316LN base plate: a root pass and a cover pass. Prepared square butt edge for LBW, FSW, and AGTAW procedures After using SiC polishing paper to remove any remaining debris, the base plates were cleaned for ten to fifteen minutes in an ultrasonic bath containing  $(\text{CH}_3)_2\text{CO}$ . A welding machine with an auto linear attachment (Miller manufacture, Model: Dynasty 350) was used to create a dual pass GTAW joint. The GTAW joint was made using a tungsten electrode with a diameter of 2.4 mm and filler wire (ER316L) with a diameter of 2 mm. Table 4.3 displays the determined optimal process parameters for several welding techniques, which were determined through trial and experimental runs.

Table 4.3 Process parameters used for different welding processes.

Parameters	Welding Process				
	GTAW		AGTAW	LBW	FSW
	Pass-1	Pass-2			
Filler wire diameter (mm)	2.4	2.4	-	-	-
Electrode diameter (mm)	2	2	2	-	-
Tip angle ( $^\circ$ )	60	60	60	-	-
Welding Current I (A)	65	64	120	-	-
Arc Voltage V (V)	12	11	12.6	-	-
Welding speed S (mm/min)	60	58	85	1500	50
Power P (kW)	-	-	-	2.5	-
Shielding gas & flow rate(l/min)	Ar/10	Ar/10	Ar/10	Ar/5	-
Spindle speed S (rpm)	-	-	-	-	600
Axial force F (kN)	-	-	-	-	14
Heat Input Q (kJ/mm)	0.780	0.790	1.067	0.100	0.636

A multi-component activated flux (a mixture of Cr<sub>2</sub>O<sub>3</sub> (10–20%), TiO<sub>2</sub> (30–50%), SiO<sub>2</sub> (25–40%), CuO (5–15%), and NiO (5–15%)) was applied to the plate that was to be welded after being dissolved in acetone to create glue similar to that used for an AGTAW connection. Using a welding equipment with an auto linear attachment, more AGTAW welding was done using the same non-consumable tungsten electrode with a diameter of 2.4 mm without the need of filler material (Miller manufacture, Model: Dynasty 350). A 3.5 kW CO<sub>2</sub> slab laser welding equipment (CIM manufacture, Model:

ML2000) was used to create the LBW joint. Base plates had a suitable purging gas arrangement for the LBW process and were firmly secured onto an indigenously manufactured fixture. The top side of the base plate was purged using argon that had a purity level of 99.995%. A single pass was used to create the LBW joint. A CNC-controlled friction stir welding equipment with three servo motors was used to create the FSW joint. As a tool material, tungsten doped with lanthanum oxide (W:99%, La<sub>2</sub>O<sub>3</sub>:1%) was employed.



Figure 4.3 LBW Machine (Facility at ARCI)



Figure 4.4 Welding machines utilized for the fabrication of the joints

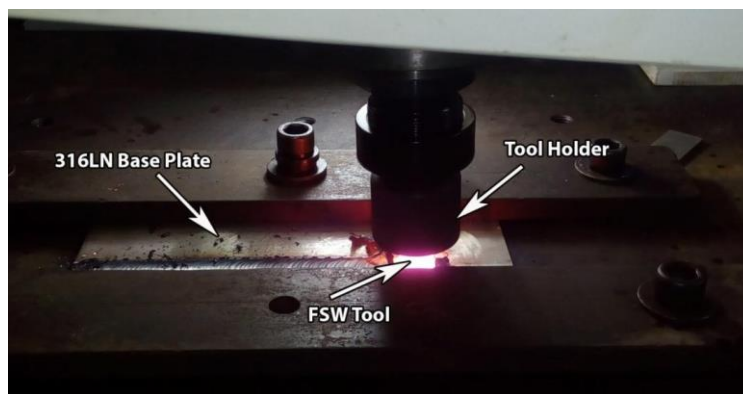


Figure 4.5 Photograph taken during Friction Stir Welding of 316LN SS

**D. EXAMPLE SETTING UP**

Figure 4.6 shows the sample extraction technique for the macrostructure of the weld zones, microstructural characterisation, mechanical property assessment, and SCC behaviour. The Wire cut Electrical Discharge Machining process was used to create all samples with the necessary dimensions. Figure 4.7a shows the dimensions that were created in accordance with ASTM E8-04 (ASTM, 2004) in order to assess transverse tensile characteristics. By evaluating all weld samples along the weld direction, the yield strength, ultimate tensile strength, and percentage of elongation of the GTAW, AGTAW, LBW, and FSW weld joints were compared with those of the base metal. Figure 4.7 b displays the longitudinal direction dimensions for all-weld subsize samples. Given that the LBW fusion zone's maximum width is significantly smaller than that of other weld joints, a flat micro tensile sample was created for the LBW weld joint along the

weld direction. Figure 4.7c displays the flat micro tensile sample's dimensions. To assess the impact toughness of the various weld joints, Charpy impact test samples with a 45oV-notch in the centre of the fusion zone were manufactured in accordance with ASTM E23-07 (ASTM, 2007) standard. Subsize Charpy impact test samples were made using 316LN plates that had been welded to a thickness of 3 mm. Figure 4.7 d displays the dimensions utilised in the Charpy impact test. Figure 4.7 e displays the dimensions of guided bend test samples for weld joints that were made in accordance with ASTM standard E190-92 (ASTM, 2008). Corrosion from Direct Tension Stress As per the ASTM G49-85 (ASTM, 2011) standard, cracking samples were manufactured, and Figure 4.7f displays their dimensions. To use lock pins to secure the sample at the top and bottom holders, a 6 mm hole was bored into the sample's grip area on both sides.

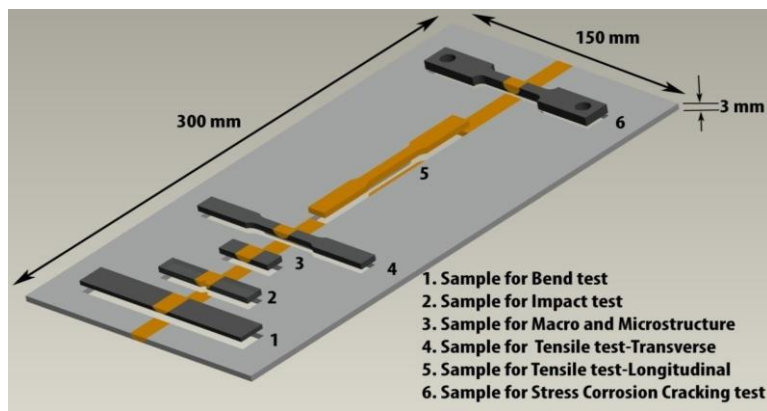
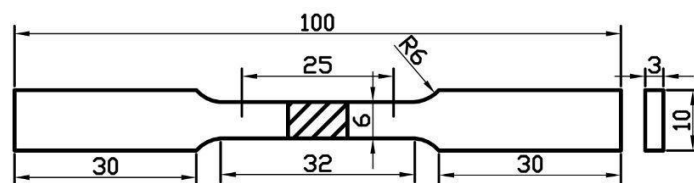


Figure 4.6 Scheme of extraction of samples for properties evaluation.

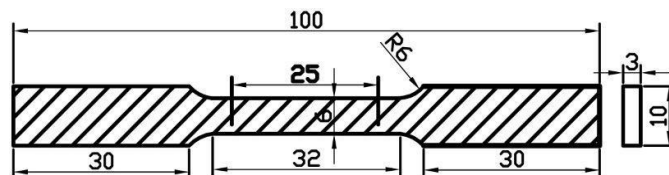
**E. CHARACTERIZATION OF AISI 316LN SS WELD JOINTS**

By obtaining samples from the transverse direction of the welded joint, the various welded connections were

metallurgically characterised. The subsequent sections provide an explanation of the specific metallurgical characterizations.



a. Tensile sample (Transverse)



b. All weld Tensile Sample (Longitudinal)

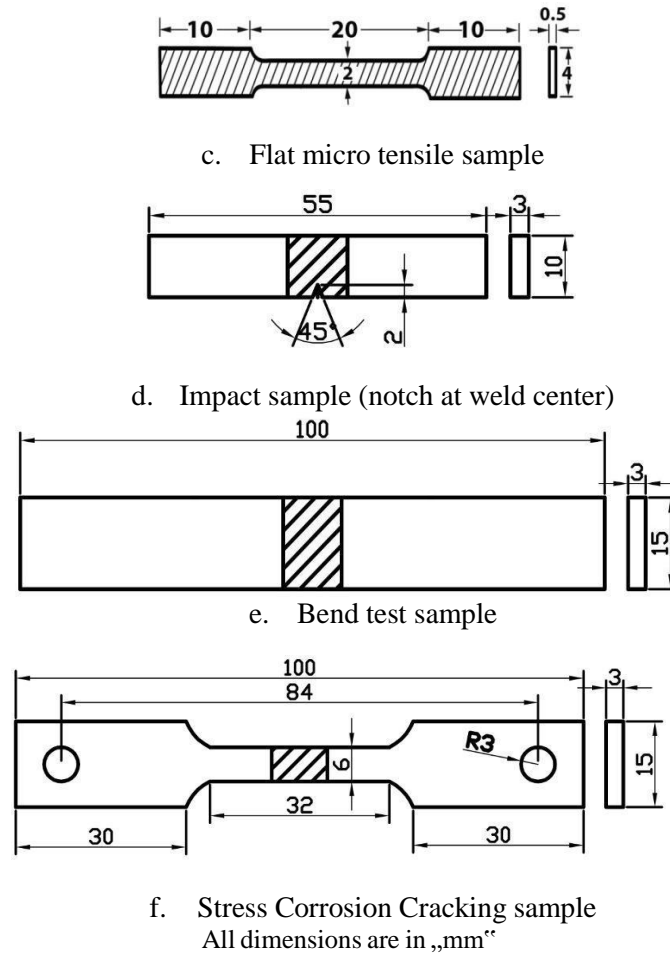


Figure 4.7 Dimensions of samples for the evaluation of mechanical properties and SCC behavior.

## F. EVALUATION OF MECHANICAL PROPERTIES

### 1) Tensile Test

The 50 KN Universal Testing Machine (Bluestar manufacture, Model: LDW 50) was used to perform the transverse tensile test on the weld samples. Tensile specimens of subsize were produced in accordance with ASTM E8-04 (ASTM, 2004). To assess the transverse tensile characteristics

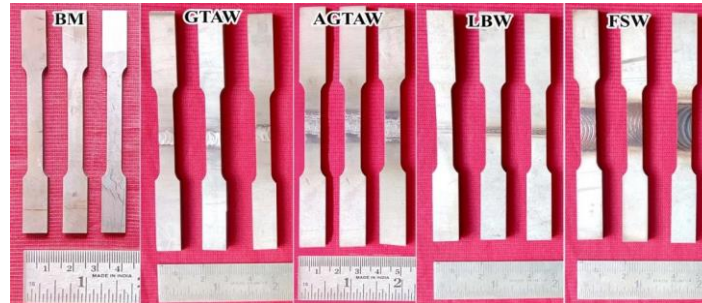
of three welded samples, tests were conducted. Throughout the tensile test, the crosshead speed of 2 mm/min was kept constant for every sample. Figure 4.8 shows the UTM used to assess the welded joint's transverse and longitudinal tensile characteristics. Figure 4.9 displays the transverse tensile samples both before and after the experiment.



Figure 4.8 Universal Testing Machine used for the tensile experiment

Furthermore, by examining all weld samples that are removed along the weld direction, the yield strength (YS), ultimate tensile strength (UTS), and the percentage of elongation of the GTAW, AGTAW, LBW, and FSW joints were compared with the base metal. Microsamples were produced at the LBW joint's restricted fusion zone along the path of the weld. Section

4.4 contains the specifics and measurements of the micro tensile samples. Furthermore, a scanning electron microscope (Model: EVO 18 research, Carl ZEISS manufacture) was used to examine the fracture surface morphology of weld joints containing base metal.



Before Experiment



After Experiment

Figure 4.9 Tensile Samples

### 2) Impact Toughness

In accordance with ASTM E23-07 (ASTM, 2007) guidelines, 45oV-notch Charpy impact test specimens were created and put through testing to determine how robust the weld joints were. An impact testing machine (FIE manufacture, Model: IT30) operated at room temperature during the impact test. Figure 4.9 displays the Charpy impact test specimens both prior to and following the test. Furthermore, a scanning electron microscope (Model: EVO 18 research, Carl ZEISS manufacture) was used to examine the fracture surface morphology of weld joints containing base metal.

### 3) Hardness of microstructure

A Vickers microhardness tester (ESEWY manufacture, Model: EW-423DAP) was used to determine the microhardness across the transverse side of the weld joints. The test was conducted at a force of 0.5 kg and a standard dwell period of 15 s. Throughout the hardness testing process, the gap between the two indentations remained constant at 0.3 mm

for every weld joint. For the GTAW, AGTAW, and LBW joints, the highest microhardness values recorded in the fusion zone were 21, 16, and 5, respectively. In the meanwhile, 31 microhardness measurements at the FSW joint's stir zone were taken.

### 4) Bend Examination

The base metal and weld joints underwent the standard guided 2T bend test, which was carried out using a 50 kN Universal Testing Machine (Bluestar manufacture, Model: LDW 50). The conventional guided bend test experimental setup is shown in Figure 4.10. The bend former has a roller with a diameter of 22 mm. For the 2T bend test, the spacing between the supports was kept at 28 mm, and two times the sample thickness (6 mm) was added with the roller diameter. The bend test samples of various welded joints are displayed both before and after the experiment in Figure 4.11.

5) *The Remaining Stress*

Using a non-destructive ultrasonic approach, the residual stress generated during the production of the welded joints was calculated. For the Critically refracted longitudinal (LCR) wave model, a custom made wave transmitter was utilised. The

transit time between the various weld joints was determined using the LCR waves. The related predicted transit time values were used to evaluate the tensile residual stress values of various welded joints.



a) Before Experiment



b) After Experiment

Figure 4.9 Impact toughness samples

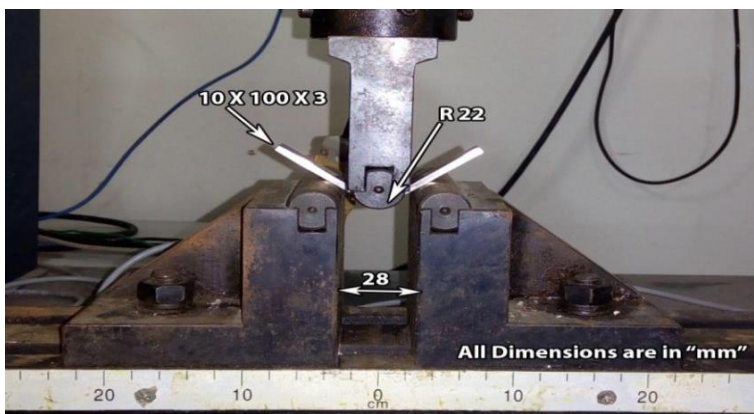
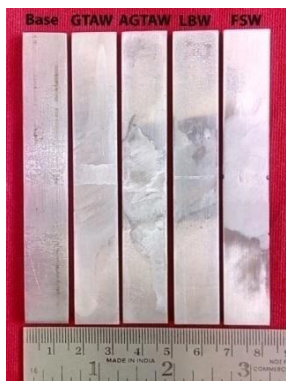
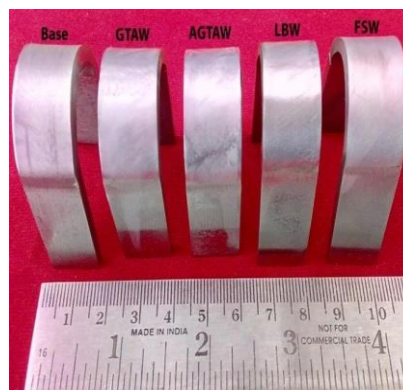


Figure 4.10 Photograph taken during bent test



a) Samples before 2T bend test



b) Samples after 2T bend test

Figure 4.11 Bend test Samples

### G. SUMMARY

The welding facilities of the Centre for Materials Joining and Research (CEMAJOR), Department of Manufacturing Engineering, Annamalai University, were utilised to fabricate the FSW joint of AISI 316LN Austenitic SS. The welding facility of ARCI, Hyderabad, India, was used to fabricate the LBW joints of AISI 316LN Austenitic SS. The facilities of the Indira Gandhi Centre for Atomic Research (IGCAR), Kalpakkam, India, and Sri Sivasubramania Nadar College of Engineering (SSNCE), Chennai, India, were used to produce AISI 316LN GTAW and AGTAW joints. The Indira Gandhi Centre for Atomic Research (IGCAR), Kalpakkam, India, facility accessible for Material Technology Division sections was used to test the microhardness, residual stress, and ferrite of welded joints.

## V. CONCLUSIONS AND SCOPE FOR FURTHER RESEARCH

### A. CONCLUSION

Based on the microstructural characterization, mechanical properties evaluation and stress corrosion cracking behavior assessment of the different welded joints, the following significant conclusions are derived.

Obtained results from this investigation can be effectively used for the Selection of welding process for 316LN austenitic stainless steel to fabricate structural components of Fast Breeder Reactors.

- The defect-free weld can be produced by all four welding techniques (GTAW, AGTAW, LBW & FSW). However, the LBW process is alone susceptible to microporosity due to the super saturation of nitrogen during rapid solidification.
- The high  $\delta$ -Ferrite content was found at the weld zone of the GTAW joint followed by the weld zone of the LBW joint. This higher  $\delta$ -Ferrite content of GTAW & LBW joints over AGTAW and FSW joints attributed to the fast cooling rate of GTAW and LBW processes. Very less amount of  $\delta$ -Ferrite content was recorded on the weld zone of the AGTAW joint.

### B. SUGGESTIONS FOR FURTHER RESEARCH

- Investigating the effect of the different filler material on the weld metal chemistry of the 316LN joints. Since the weld metal chemistry is one of the key factors for mechanical and SCC behavior.

- Conducting the comparison of the chloride-induced SCC on the 316LN welded joint using different environments such as NaCl and HCl.
- Investigating the effect of welding processes on SCC behavior of 316LN joints welded using Slow Strain Rate Testing (SSRT) and making performance index.
- Investigating the effect of welding processes on SCC behavior of 316LN joints welded using the following configurations: (i) Pipe joints (ii) Tube to tube plate and (iii) T-joints since the formation of the residual stress will be high for T-joints case.

## REFERENCES

- [1] Ahmadi, E & Ebrahimi, AR 2015, „Welding of 316L austenitic stainless steel with activated tungsten inert gas process“, Journal of materials engineering and performance, vol. 24, no. 2, pp. 1065-1071.
- [2] Alali, M, Todd, I & Wynne, BP 2017, „Through-thickness microstructure and mechanical properties of electron beam welded 20 mm thick AISI 316L austenitic stainless steel“, Materials & Design, vol. 130, pp. 488-500.
- [3] Alwin, B, Lakshminarayanan, AK, Vasudevan, M & Vasantharaja, P 2017, „Assessment of Stress Corrosion Cracking Resistance of Activated Tungsten Inert Gas-Welded Duplex Stainless Steel Joint“, Journal of Materials Engineering and Performance, vol. 26, pp. 12, pp. 5825-5836.
- [4] Alyousif, OM & Nishimura, R 2007, „On the SCC behaviour of austenitic stainless steels in boiling saturated magnesium chloride solution“, WIT Transactions on Engineering Sciences, vol. 54, pp. 257-266.
- [5] ASTM E190-92 2003, Standard Test Method for Guided Bend Test for Ductility of Welds, ASTM International, West Conshohocken, PA, 2003, www.astm.org.
- [6] ASTM E23-07, Standard Test Methods for Notched Bar Impact Testing of Metallic Materials, ASTM International, West Conshohocken, PA, 2007, www.astm.org.
- [7] ASTM E407-07 2015 e1, Standard Practice for Microetching Metals and Alloys, ASTM International, West Conshohocken, PA, 2015, www.astm.org
- [8] ASTM E8-04, 2004 Standard Test Methods for Tension Testing of Metallic Materials, ASTM International, West Conshohocken, PA, www.astm.org
- [9] ASTM G36-94 2018, Standard Practice for Evaluating Stress-Corrosion-Cracking Resistance of Metals and Alloys in a Boiling Magnesium Chloride Solution , ASTM International, West Conshohocken, PA, 2018, www.astm.org.
- [10] ASTM G49-85 2019, Standard Practice for Preparation and Use of Direct Tension Stress-Corrosion Test Specimens, ASTM International, West Conshohocken, PA, 2019, www.astm.org.